

A Physically Based Model for Predicting Volume Shrinkage in Chemically Amplified Resists

Nickhil Jakatdar¹, Junwei Bao, Costas J. Spanos

Dept. of Electrical Engineering and Computer Sciences, University of California, Berkeley, CA 94720

Ramkumar Subramanian, Bharath Rangarajan

Advanced Micro Devices, Sunnyvale, CA 95052

Andy Romano

70 Meister Avenue, AZ division-Clariant Corporation, Somerville, New Jersey, NJ 08876

ABSTRACT

Improvements in the modeling of chemically amplified resist systems are necessary to extract maximum possible information from limited experimentation. Previous post-exposure bake models have neglected volume shrinkage, thus violating the continuity equations used to model the process. This work aims at describing the kinetics of the post-exposure bake process by tracking the volume shrinkage observed in both low and high activation energy resists. Both static and dynamic models are derived and corroborated with experimental results for Shipley UV5 and AZ 2549 resists. A global simulation technique is then used in conjunction with the models to extract the lithography parameters for these resists.

Keywords: Deprotection Induced Thickness Loss (DITL), Adaptive Simulated Annealing (ASA), Chemically Amplified Resists, Prolith,

1. INTRODUCTION

As we enter the DUV lithography generation, the developmental phase of the photolithography process is becoming crucial due to the high costs associated with equipment and materials, and the continually shortened time-to-market. Improvements in the modeling of chemically amplified resists are necessary to extract the maximum possible information from least amount of experimentation. All chemically amplified resist systems exhibit a significant volume shrinkage either during the exposure or post-exposure bake process (typically 4% to 15% in current resist systems) [1]. Current models for PEB and development do not take into consideration this shrinkage for calculating line-widths. At present, workers at AMD [2] are developing a new methodology for characterizing PEB. Adding shrinkage characterization to the understanding of bake and development will significantly improve our understanding of lithography resist processing. This volume shrinkage manifests itself in the form of thickness loss and it has been shown that this shrinkage is directly proportional to the deprotection of the resist in flood exposed films [3].

This work aims at describing the kinetics of the post-exposure bake process by tracking the volume shrinkage observed in both low and high activation resists. We begin with a brief introduction of the physical mechanism underlying the volume shrinkage followed by the proposed equations for both the static model as well as the dynamic model. An optimization framework is then

1. Further author information -

N.J. (correspondence): Email: nickhil@eecs.berkeley.edu; WWW: <http://radon.eecs.berkeley.edu/~nickhil>; Telephone: (510) 642-9584;

Fax:

(510) 642-2739

presented that is used to extract the parameters of the models. Finally, results of modeling two different resists are discussed.

2. BACKGROUND

Chemically Amplified Resists (CARs) are typically composed of a polymer resin, which is very soluble in an aqueous base developer, a protecting t-BOC group, resulting in a very slowly dissolving polymer, photo-acid generators and possibly some dyes and additives along with the casting solvent. The deprotection mechanism can be broken down into the initiation, the deprotection and the quenching stages. In the initiation phase, the exposure energy causes the Photo-Acid Generator (PAG) to produce acid. In the deprotection phase, these H^+ ions attack the side chains (t-BOC) of the polymer and generate more H^+ ions, making the resist even more soluble as illustrated in Figure 1. This takes place in the presence of heat. In the quenching stage, the H^+ ions are slowly quenched by anything more basic than the acid, such as the additives and the by-products of the reaction. The cleaved t-BOC is volatile and evaporates, causing film shrinkage in the exposed areas. The extent of this exposed photoresist thinning is dependent on the molecular weight of the blocking groups.

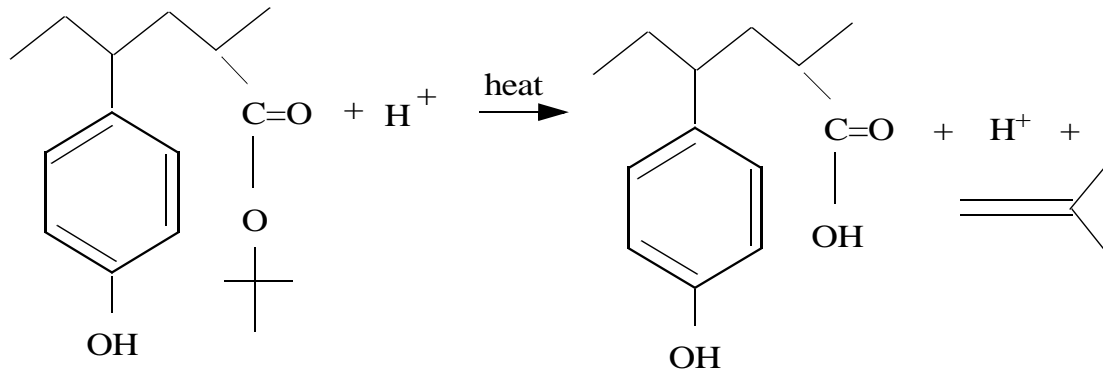


FIGURE 1. Resist Mechanism during the Exposure and Post Exposure Bake Steps for a DUV chemically amplified photoresist.

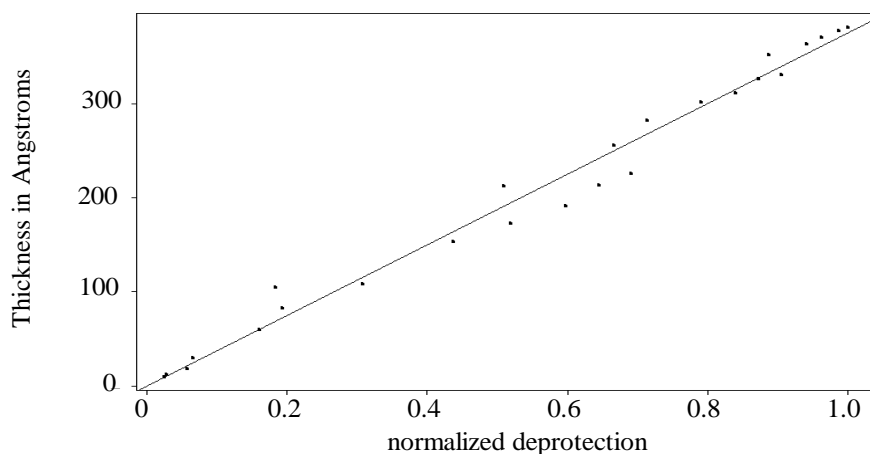


FIGURE 2. Thickness loss as a function of the deprotection measured by monitoring the normalized ester absorbance.

An experiment was performed to correlate the deprotection of the resist, as measured by Fourier Transform Infrared Spectroscopy, to the observed volume shrinkage as shown in Figure 2. The results show that the intrinsic reaction mechanism occurring in the resist during the bake could be observed through the volume shrinkage. The next logical step then would be to observe this shrinkage in real time and attempt to understand the reaction mechanism occurring in the resist.

2.1 Dynamic Model for Thickness Loss

2.1.1 Physical Models

One of the underlying assumptions in modeling the latent image through continuity equations has been that the resist volume remains constant. Ignoring the volume shrinkage would obviously reduce the accuracy of previous models. The goal of this model is to attempt to describe the physical processes occurring in the resist during the PEB step for 1-dimensional (flood) exposures, in the presence of the volume shrinkage. We begin with a description of the physical mechanisms occurring in the process, and then provide mathematical expressions to represent these physical processes.

We propose the following mechanism: During the exposure step, the photo-acid generators produce acid with normalized concentration u . The initial 1-d distribution of the acid within the resist depends on the optical constants of the resist and underlying film at the exposure wavelength. With sufficient thermal energy, the acid molecules begin to diffuse with diffusivity D_u (nm²/sec) and attack the polymer side chains. There is also an acid loss mechanism due to recombination with parasitic bases at a rate k_{loss} (1/sec). The acid diffusion is widely believed to be an exponential function of the free volume [4] with a pre-exponent term D_{u0} (nm²/s) and an exponent term a . The deprotection reaction has a rate k_2 (1/s), which has an Arrhenius relationship with temperature. The deprotection v is a normalized quantity between 0 and 1. The deprotected molecules are volatile and this normalized concentration of volatile molecules w begin to diffuse with diffusivity D_w (nm²/sec) through the resist, until it escapes the resist bulk from the top. The amount of molecules that escape would depend on the partial pressure in the wafer track. Each escaped volatile molecule leaves behind a vacancy or hole h that begins to collapse at a rate k_3 (1/sec) specific to the particular polymer. It is the polymer relaxation process that eventually causes the volume shrinkage of ϖ (nm) in the resist. Since the deprotection is a normalized quantity, a scaling factor k_1 is needed to convert the deprotection into a corresponding volatile group concentration. Similarly, a scaling factor k_4 is needed to convert the hole concentration into a corresponding volume shrinkage, to take into account the area of the flood exposed site. All the concentrations are normalized to the initial photo-acid generator concentration and are hence unitless. In the case of low activation energy resist systems, this mechanism begins during the exposure step itself, while in the case of high activation energy systems, this process begins to occur only during the PEB step.

The mechanism described above can be described with the following six equations:

$$\frac{\partial}{\partial t}(u\varpi) = \nabla \bullet (D_u \nabla u)\varpi - k_{loss}u\varpi \quad (1)$$

$$\text{where } D_u = D_{u0} \exp(ah) \quad (2)$$

$$\frac{\partial v}{\partial t} = k_2 u (1 - v) \quad (3)$$

$$\frac{\partial}{\partial t}(w\varpi) = [D_w \nabla^2 w + k_1 k_2 u(1-v)]\varpi \quad (4)$$

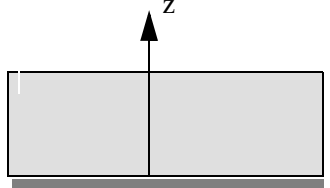
$$\frac{\partial}{\partial t}(h\varpi) = [-D_w \nabla^2 w - k_3 h]\varpi \quad (5)$$

$$\frac{\partial \varpi}{\partial t} = -k_4 k_3 h \varpi \quad (6)$$

Eq. 1 suggests that the rate of change of acid concentration at any point in the resist is governed by the non-linear acid diffusion within the resist caused by the acid gradient that exists at that point. This gradient in turn exists due to changing exposure conditions in the film, caused by internal reflectance and absorbance of light by the resist film during exposure. The acid diffusion is modeled by Eq. 2. Eq. 3 represents the rate of normalized deprotection reaction and is proportional to the amount of acid and the amount of unreacted sites. Eq. 4 indicates that the rate of change of volatile groups within an infinitesimal volume element is proportional to the number of volatile groups diffusing through the volume element and the generation rate is proportional to the normalized deprotection rate. Eq. 5 represents the rate of change of holes (or free volume). The generation rate of holes within any infinitesimal volume element depends on the number of volatile groups diffusing out of that volume element while the destruction rate of holes within that same volume element is dependent on the polymer relaxation rate constant. Eq. 6 models the volume shrinkage within each volume element and is proportional to the free volume relaxation rate. The ϖ term is included in all the equations that deal with concentrations, to account for the changing volume.

2.1.2 Boundary Conditions

The logical next step is to define the boundary conditions for this problem. They would be as follows:



$$\frac{\partial u}{\partial z} \Big|_{top} = 0 \quad (7)$$

$$\frac{\partial w}{\partial z} \Big|_{bottom} = 0 ; w \Big|_{top} = 0 \quad (8)$$

$$u \Big|_{t=0} = u_0(z) \quad (9)$$

where $u_0(z) = 1 - \exp(-cD(z))$ and

$$D(z) = D_0 \left[\exp(-\alpha z) + |r|^2 \exp(-\alpha(2d-z)) - 2|r| \exp(-\alpha d) \cos\left(\frac{4\pi n}{\lambda}(d-z)\right) \right] \quad (10)$$

where the D_0 is the applied dose corrected by the reflectivity at the air-resist interface, α is the linear absorbance of the resist film, d is the film thickness, n is the real part of the refractive index, λ is the exposure wavelength, C is the acid production rate and r is the reflectivity coefficient of the resist/substrate interface.

$$h \Big|_{t=0} = h_0 \quad (11)$$

$$v|_{t=0} = w|_{t=0} = 0 \quad (12)$$

Eq. 7 indicates that there is no acid loss due to evaporation at the resist surface. However, this condition can easily be modified to model T-topping or environmental contamination. Eq. 8 indicates that the volatile group escapes from the resist only at the resist-air interface and this gradient is facilitated by maintaining the volatile group concentration at the resist-air interface at zero. Eq. 9 states that the initial acid distribution during exposure is determined by the aerial image and the optical properties of the resist, given in Eq. 10. Eq. 11 refers to the presence of an initial free volume concentration in the resist, which is a function of the spin-on and soft bake process [5]. Eq. 12 states that the deprotection and volatile group concentrations at the beginning of the PEB process are zero (for low activation energy resist systems, this would be a value greater than zero).

2.1.3 Computational Approach

A finite difference system was set up for numerically solving the equations subject to the boundary conditions described above. A simple forward difference technique (explicit method) was used to step the equations in time with sufficient time and space steps to avoid numerical instability problems [6]. We used 200 space steps (1 step = 3.25 nm) and 5000 time steps (1 step = 16 ms of baking time) in our computation, yielding 10 seconds for simulating a thickness loss versus time set for a given dose. An implicit method such as the Crank-Nicholson method [6] would have allowed for fewer time and space steps, but would require computation time intensive matrix computations to solve the simultaneous equations.

2.2 Static Model for Thickness Loss

Static models are useful in cases when experimental data is available only at a fixed PEB time, which is typically the case. The deprotection induced thickness loss at different doses can be used in conjunction with a model of the PEB process to extract relevant simulation parameters, such as the Dill's C parameter, the relative quencher concentration Q , the amplification reaction rate (E_{amp} , A_{amp}), etc. Currently, there exists no model for the bake process that can capture the deprotection "S" curve through multiple doses and temperatures. Current models are insufficient, because they incorrectly assume that the acid quencher remains constant throughout the bake process. In our model, we assume that during the PEB process, acid is lost in neutralization reactions with bases that are either designed into the resist or exist as unreacted portions of the polymer. This indicates that the bases will also correspondingly reduce with time, and the difference between the acid and base concentrations will remain constant throughout the PEB process. We model the above mechanism with Eq. 13 and Eq. 14.

$$\frac{\partial}{\partial t}[Acid] = -k_\alpha[Acid][Q] \quad (13)$$

$$[Acid]_t - [Q]_t = Const = [Acid]_0 - [Q]_0 \quad (14)$$

where α is the neutralization reaction rate (1/sec) modeled by an Arrhenius for temperature, $[Q]$ is the normalized quencher concentration and $[Acid]$ is the normalized acid concentration. Both the quantities are normalized to the initial photo-acid generator concentration. The initial value for quencher $[Q]_0$ is a parameter that can be extracted from the experimental data using the procedure outlined in Section 2.3, while the initial acid concentration $[Acid]_0$ is obtained from Eq. 15. [7]

$$[Acid]_{dose} = [PAG]_0(1 - e^{-C \times dose}) \quad (15)$$

Solving the above equations yields the following analytical solution for the acid concentration as a function of the PEB time:

$$[Acid]_t = \frac{([Acid]_0 - [Q]_0)}{1 - \frac{[Q]_0}{[Acid]_0} \exp(-k_\alpha([Acid]_0 - [Q]_0)t)} \quad (16)$$

Meanwhile, the deprotection reaction is typically modeled by Eq. 17, where k_{amp} (1/sec) is the reaction amplification coefficient and is modeled by an Arrhenius relationship as a function of temperature.

$$\frac{\partial}{\partial t}[M] = -k_{amp}[Acid]_t[M] \quad (17)$$

Substituting Eq. 16 in Eq. 17 and solving for the normalized concentration of unreacted blocking sites m , we get

$$\frac{[M]_t}{[M]_0} = m = \left[\frac{[Acid]_0 e^{(k_\alpha([Acid]_0 - [Q]_0)t)} - [Q]_0}{[Acid]_0 - [Q]_0} \right]^{-\frac{k_{amp}}{k_\alpha}} \quad (18)$$

Eq. 18 differs from previous work in that it accounts for the fact that the bases (both parasitic and designed) are consumed in the neutralization reaction. Getting rid of the earlier simplifying assumption now allows us to better model the initial delay in deprotection increase with exposure dose, and hence provides an estimate of the relative quencher concentration $[Q]_0$ as well.

2.3 Parameter Extraction Framework

Having a model to represent a process allows the use of an optimization engine to extract the parameters of the model from experimental data. However, due to the high dimensionality and non-linearity of the problem, traditional optimization approaches do not perform as well. We propose using a stochastic global optimizer such as Simulated Annealing (SA) [8] to overcome this problem. While this approach does not guarantee convergence to the global minima, it has provided encouraging results in past applications to lithography simulations [9]. The block diagram for the optimization process is shown in Figure 3. The dose distribution into the resist and the conversion of the dose into acid is done using Eq. 10. This initial acid distribution is fed along with the first set of resist parameters generated by the optimization engine, to the 1-d volume shrinkage simulator. The output of the simulator is compared with the experimental data, the resulting error is fed to SA and a new set of parameters is generated. This process continues until the sum squared error between the model prediction and experimental data reduces below a pre-determined threshold value.

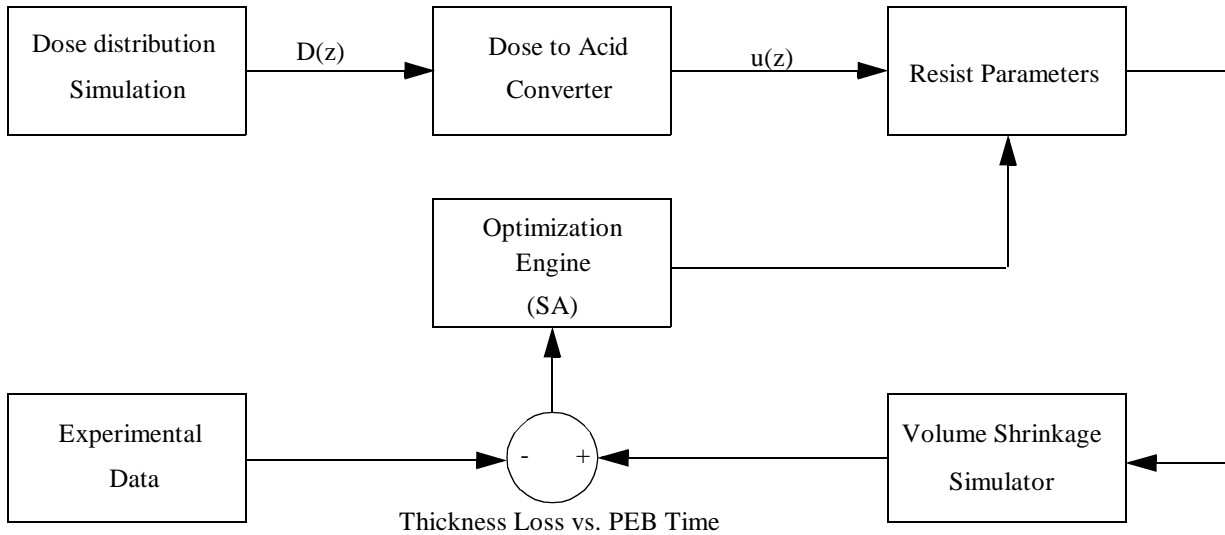


FIGURE 3. Block diagram for resist parameter extraction from the dynamic model and experimental data.

3. EXPERIMENTAL

Two sets of experiments were done. In the first set, Shipley's UV-5 resist was processed at 60 different exposure doses and 5 different PEB times at the standard conditions. The wafers were measured for thickness before exposure and after PEB. This data set provided values for thickness loss at 5 discrete times, as well as inputs for the static model. The other experiment involved measuring the thickness loss in real time during the PEB process for 2 wafers for the AZ 2549 resist. A commercial reflectometer was used for the real time measurements, while an ellipsometer was used for the static thickness measurements.

4. RESULTS AND DISCUSSION

We begin with results of the dynamic model fitting to the experimental data for UV-5, AZ 2549. Figure 4 shows the results for UV-5 while Figure 5 shows the results for AZ 2549.

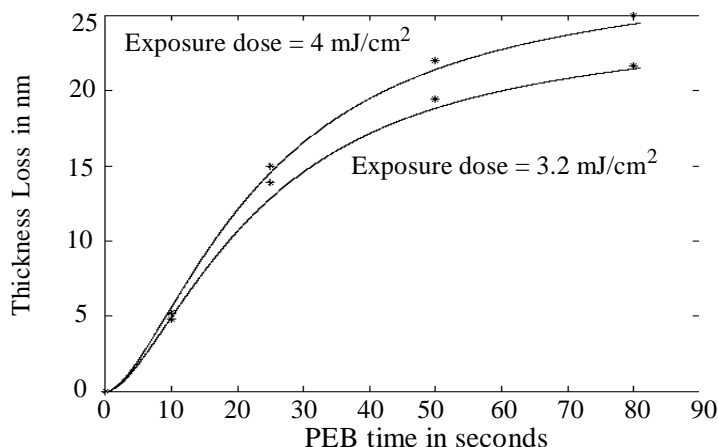


FIGURE 4. Measurements of thickness loss versus time for UV-5 at 130 degrees C. Measured values are shown as *

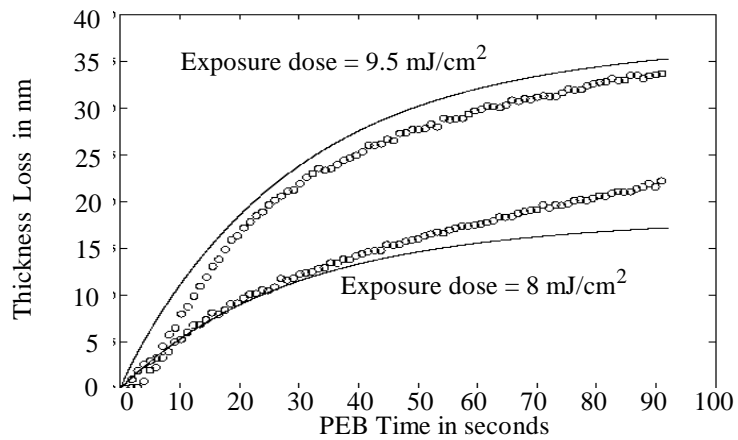


FIGURE 5. Measurements of thickness loss versus time for AZ 2549 at 110 degrees C. Measured values shown in o

Figure 6 shows the results of fitting the static model to experimental data for UV-5 while Figure 7 shows the results of fitting the static model to experimental data for AZ-2549.

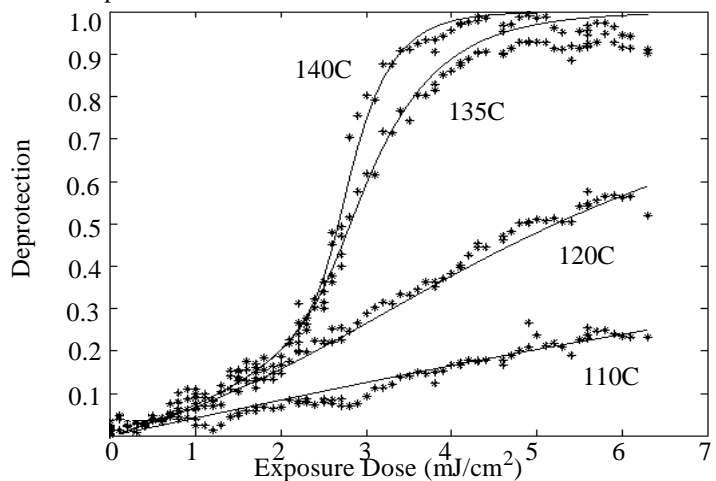


FIGURE 6. Static model fitting experimental data for UV-5. Measured values are shown as *

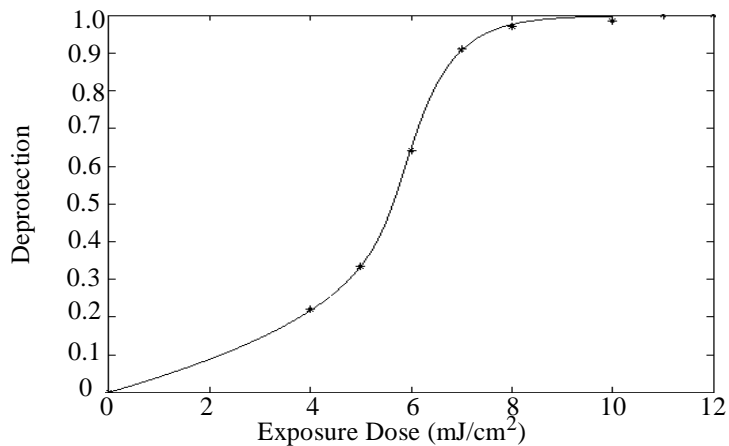


FIGURE 7. Static Model fitting experimental data for AZ-2549 at 110 deg. C. Measured values are shown as *

We tabulate the results for UV-5 and AZ-2549 below.

Parameter	UV-5	AZ 2549
K_{amp} (1/sec) at 130C	0.3406	0.228
K_α (1/sec) at 130C	1.16	2.55
C (cm ² /mJ)	0.059	0.0123
[Q] (normalized quantity)	0.177	0.049

5. CONCLUSIONS

In the preceding sections, we have proposed both static and dynamic physical models for volume shrinkage in chemically amplified resists. The static model successfully models the quenching action in the resist across the complete exposure dose spectrum and in the process, extracts critical resist parameters used in commercial lithography simulators. The proposed dynamic model successfully predicts the volume shrinkage observed in resists and could be used to gain insight into the resist mechanism.

6. ACKNOWLEDGEMENTS

This work was supported by the MICRO under 97-167 and also by UC-SMART under MP 97-1.

7. REFERENCES

- [1] C. A. Mack, "Inside Prolith - A Comprehensive Guide to Optical Lithography Simulation", February 1997
- [2] Capodieci, et. al., "A novel methodology for post-exposure bake calibration and optimization based on electrical linewidth measurements and process metamodeling", EIPB Conference, May 1998
- [3] N. Jakatdar, et.al. "Characterization of a Positive Chemically Amplified Photoresist from the Viewpoint of Process Control for the Photolithography Sequence", SPIE vol. 3332, pp.586-593, 1998
- [4] M. Zuniga, A.R. Neureuther, "Reaction-Diffusion Modeling and Simulations in Positive DUV Resists", JVST-B, Nov-Dec 1995, vol. 13, pp. 2957-62
- [5] L. Pain, et.al., "Free Volume Effects in Chemically Amplified DUV Positive Resists", Microelectronic Engineering 30 (1996) pp. 271-274
- [6] W. Vetterling, et. al., "Numerical Recipes for C", 2nd edition, 1992
- [7] J. Byers, et.al., "Characterization and Modeling of a Positive Chemically Amplified Resist", SPIE vol. 2438, pp.153-166, 1995
- [8] L. Ingber, "Simulated Annealing", <ftp://alumni.caltech.edu/pub/ingber/>, 1995
- [9] N. Jakatdar, et.al., "Characterization of a Chemically Amplified Photoresist for Simulation using a Modified Poor Man's DRM Methodology", SPIE vol. 3332, pp.578-585, 1998